

RESEARCH

Open Access



Investigation on taxonomy, secondary metabolites and antibacterial activity of *Streptomyces sediminicola* sp. nov., a novel marine sediment-derived *Actinobacteria*

Kun Zhang^{1,2†}, Wenping Ding^{1†}, Chenghui Han¹, Lijuan Long^{1,3}, Hao Yin^{1*} and Jianping Yin^{1,3*}

Abstract

Background Marine actinomycetes, especially *Streptomyces*, are recognized as excellent producers of diverse and bioactive secondary metabolites on account of the multiplicity of marine habitations and unique ecological conditions, which are yet to be explored in terms of taxonomy, ecology, and functional activity. Isolation, culture and genome analysis of novel species of *Streptomyces* to explore their potential for discovering bioactive compounds is an important approach in natural product research.

Results A marine actinobacteria, designated strain SCSIO 75703^T, was isolated, and the potential for bioactive natural product discovery was evaluated based on genome mining, compound detection, and antimicrobial activity assays. The phylogenetic, phenotypic and chemotaxonomic analyses indicate that strain SCSIO 75703^T represents a novel species in genus *Streptomyces*, for which the name *Streptomyces sediminicola* sp. nov. is proposed. Genome analysis revealed the presence of 25 secondary metabolite biosynthetic gene clusters. The screening for antibacterial activity reveals the potential to produce bioactive metabolites, highlighting its value for in-depth exploration of chemical constituents. Seven compounds (**1–7**) were separated from the fractions guided by antibacterial activities, including three indole alkaloids (**1–3**), three polyketide derivatives (**4–6**), and 4-(dimethylamino)benzoic acid (**7**). These primarily antibacterial components were identified as anthracimycin (**4**), 2-*epi*-anthracimycin (**5**) and β -rubromycin (**6**), presenting strong antibacterial activities against Gram-positive bacteria with the MIC value ranged from 0.125 to 16 μ g/mL. Additionally,, monaprenylindole A (**1**) and 3-cyanomethyl-6-prenylindole (**2**) displayed moderate inhibitory activities against α -glucosidase with the IC₅₀ values of 83.27 and 86.21 μ g/mL, respectively.

Conclusion Strain SCSIO 75703^T was isolated from marine sediment and identified as a novel species within the genus *Streptomyces*. Based on genomic analysis, compounds isolation and bioactivity studies, seven compounds were identified, with anthracimycin and β -rubromycin showing significant biological activity and promising potential for further applications.

Keywords *Streptomyces sediminicola* sp. nov., Secondary metabolites, Structural elucidation, Anti-bacterial activity

[†]Kun Zhang and Wenping Ding These authors contributed equally to this work.

*Correspondence:

Hao Yin

yinhao@scsio.ac.cn

Jianping Yin

yjp@scsio.ac.cn

Full list of author information is available at the end of the article



Background

Marine actinomycetes have attracted considerable attention due to their ability to produce a diverse array of biologically active secondary metabolites, which have remained powerful forces driving pharmaceutical discovery [1]. Since the discovery of streptomycin in 1943, research on actinomycetes has seen tremendous growth, ushering in a golden period for the discovery of new natural products [2, 3]. While the frequent rediscovery of known secondary metabolites from the *Streptomyces* species has diverted some scientists' attention to rare actinomycetes [4], the influence of environmental conditions and diverse habitats strongly contribute to the production of novel secondary metabolites with diverse structures and bioactivities. The genus *Streptomyces* is ubiquitous in terrestrial and marine environments and is known for a rich source of bioactive natural products, especially antibiotics [5, 6]. In particular, marine *Streptomyces* are able to produce unique secondary metabolite profile distinct from terrestrial *Streptomyces*, owing to their unique habitats under harsh conditions such as high pressure, high salinity, nutrient deficiency and lack of oxygen [5, 7]. The highlights involve in the production of secondary metabolites such as antibiotics, anticancer compounds, enzyme inhibitors and pigments [8].

The advent of high-throughput metagenomic sequencing has expanded our knowledge and revealed the presence of numerous novel actinomycetes that were previously undetected in cultivation studies [9]. Therefore, isolating and identifying novel *Streptomyces* resources from marine environments is beneficial for discovering active metabolites. In addition, with the advancements in whole-genome sequencing and bioinformatics analysis, it has been revealed that marine *Streptomyces* possess immense potential for synthesizing secondary metabolites has been substantially underestimated [7]. The integration of genome mining as a strategic approach has greatly facilitated the discovery of natural products through the analysis of secondary metabolite biosynthetic gene clusters (BGCs) and biosynthetic pathways [7].

In this study, we aimed to highlight the key findings from our taxonomic and chemical investigations of sediment-derived *Streptomyces*. Using a polyphasic taxonomic approach, we characterized a novel species of *Streptomyces*, designated SCSIO 75703^T, isolated from marine sediment. In our ongoing search for secondary metabolites with chemical structure and potent biological activity from marine *Streptomyces*, the chemical constituents of strain SCSIO 75703^T were investigated combining with genome mining and One Strain Many Compounds (OSMAC) approach. The results from this

study provide valuable novel *Streptomyces* resource for this discovery of active compounds.

Methods

Isolation and maintenance

Strain SCSIO 75703^T was isolated from a sediment sample collected at a depth of 21 m from Wanshan marine ranching in the Pearl River Estuary (21°56'51"N, 113°38'15"E). The samples were serially diluted with sterile seawater and transferred onto 20% (w/v) 2216E agar (Hopebio) and incubated at 28 °C for 2 weeks. The isolates were picked to 2216E agar (Hopebio) and the pure cultures were preserved in glycerol suspensions (30%, v/v) at -80 °C.

16S rRNA gene phylogeny

Genomic DNA extraction and PCR amplification of the 16S rRNA gene were performed according to the methods described by Li et al. [10] with the universal bacterial primers 27F (5'-AGAGTTTGATCCTGGCTCAG-3') and 1492R (5'-GGTTACCTTGTTACGACTT-3'). Sequences similarity analysis of strains were conducted using the EzBioCloud server (www.ezbiocloud.net/identify) [11]. Multiple sequence alignments and phylogenetic reconstructions of 16S rRNA genes were carried out in MEGA version 11 and the relationships among taxa were established by using the neighbour-joining [12], maximum-likelihood [13] and maximum-parsimony algorithms [14], respectively [15].

Whole genome sequencing, annotation and analysis

The complete genome sequence (accession number: CP144555) was obtained using the Nanopore sequence platform at Guangdong Magigen Biotechnology (Guangzhou, China). Sequence assembly was performed with the PacBio SMRT analysis version 5.1.0 platform using Unicycler software (<https://github.com/rrwick/Unicycler/>) [16]. The quality of microbial genome was assessed using the bioinformatic tool CheckM [17]. The average nucleotide identity (ANI) was calculated using the ANI Calculator (<https://www.ezbiocloud.net/tool/ani/>) [18]. Digital DNA-DNA hybridization (dDDH) value was calculated using the Genome-to-Genome Distance Calculator 3.0 (<https://ggdc.dsmz.de/ggdc.php/>) [19]. The average amino acid identity (AAI) was estimated using the AAI calculator tool (<http://enve-omics.ce.gatech.edu/>) [20]. Genome phylogenetic trees were constructed using MEGA version 11 [15] by using the neighbour-joining [12] based on the 120 single-copy genes with the GTDB-Tk software toolkit [21]. The whole genome and orthologous genes analysis were compared using OrthoVenn 3 [22]. Synteny analysis of the genomes with their closest related type strains were conducted using

progressive Mauve tool [23] Biosynthetic gene clusters for secondary metabolites were predicted using the antiSMASH program (version 7.0) [24].

Phenotypic properties

Cell morphology was observed using a scanning electron microscope (Hitachi S3400N) after growing cells on 2216E agar at 28 °C for 3 days. Anaerobic growth was determined after 14 days of incubation at 28 °C using the GasPak EZ anaerobic bag system (BD). Cell motility was examined by microscopic observations and inoculation on semisolid 2216E medium with 0.4% agar (w/v) [25]. Strain growth was evaluated on 2216E agar (Hopebio), Reasoner's 2A agar (R2A; Difco), nutrient agar (NA; Difco), tryptic soy agar (TSA; Difco), International *Streptomyces* Project 2, 3, 4, 5 and 7 (ISP2, 3, 4, 5 and 7; Difco) media, with incubation at 28 °C for 7 days. The temperature range for growth was determined using 2216E agar (Hopebio) at 4, 8, 15, 20, 25, 28, 30, 35, 37, 45, and 50 °C. The pH tolerance for growth was evaluated in 2216E broth across a pH range of 4.0–13.0 (1.0 pH unit interval), using buffer systems [0.1 M Citric Acid/ 0.1 M Sodium Citrate (pH=4–5), 0.1 M KH₂PO₄/0.1 M NaOH (pH=6–8), 0.1 M NaHCO₃/0.1 M Na₂CO₃ (pH=9–10), 0.2 M KCl/0.1 M NaOH (pH=11–13)]. NaCl tolerance was determined with cultivation at 28 °C in modified 2216E agar (pH 7.0, without NaCl) with NaCl supplemented at concentrations of 0–10.0% (w/v) at increasing increments of 1.0%. Hydrolysis of starch, cellulose, gelatin, and Tweens (20, 40, 60, and 80) and H₂S production, coagulation, and peptonization of milk were performed using the methods previously described [26]. Catalase activity was tested by observing bubble production in hydrogen peroxide solution (v/v, 3%) and oxidase activity was tested using oxidase reagent (bioMérieux, Marcy-l'Étoile, France). In addition, biochemical characteristics including enzymatic activities, carbon and energy source utilization were analyzed using API ZYM (bioMérieux, Marcy-l'Étoile, France), API 20NE (bioMérieux, Marcy-l'Étoile, France), and Biolog GEN III MicroPlates (Biolog, CA, USA) following the manufacturers' instructions.

Chemotaxonomic analysis

For chemotaxonomic analyses, biomass was harvested from cultures cultivated in 2216E broth for 7 days at 28 °C. Menaquinones were extracted from freeze-dried biomass as previously described [27] and analysed using HPLC [28]. The cell-wall diamino acid and whole-cell sugar were identified according to the procedures developed by Lechevalier et al. [29] and Stanek & Roberts [30], respectively. Cellular fatty acids were extracted and evaluated using the Microbial Identification System (version 6.1; MIDI database TSBA6, MIDI, Newark,

America). The polar lipids were extracted, detected with two-dimensional TLC silica gel 60F254 thin-layer plates (10×10 cm), and analyzed, as previously described [31].

General procedures

HRESIMS was measured on a Bruker maxis quadrupole-time-of-flight mass spectrometer. UV spectra were performed on a Shimadzu UV-2600 spectrophotometer. IR spectra were run on an IR Affinity-1 spectrometer (Shimadzu, Japan). ¹H, ¹³C and 2D NMR spectra were recorded on Bruker AV500 or Bruker AVIII HD 700 MHz spectrometer (Bruker, Billerica, MA, USA) using TMS as the internal standard. Chemical shifts (δ) are expressed in ppm relative to the TMS signals. Column chromatography (CC) was performed with C-18 gel (20–40 μm, Agela Technologies) and Sephadex LH-20 (100–200 μm, Pharmacia). Analytic and Semi-preparative HPLC were run on an Agilent 1260 liquid chromatograph equipped with a DAD detector with YMC-Pack ODS-A (250×4.6 mm or 250×10.0 mm, 5 μm) column, YMC-Pack Ph (250×4.6 mm or 250×10.0 mm, 5 μm) column.

Fermentation, extraction and isolation

Initially, strain SCSIO 75703^T was cultivated in eleven different liquid media (Table S1). MC3 liquid medium was selected on basis of the results of both HPLC profiles and antibacterial zones. The strain was cultivated in 500 mL Erlenmeyer flasks each containing 200 mL of MC3 culture broth at 28 °C for 7 days with shaking rate at 180 rpm to produce a total of 30 L fermentation. The culture (30 L) was extracted for three times with an equal volume of EtOAc at room temperature. The EtOAc layer was separated from the aqueous phase and was evaporated in vacuo to dryness to give an EtOAc extract (2.5 g). Subsequently, the EtOAc extract was subjected to MPLC (Cheetah MP200 Flash Purification Systems, Agela Technologies) C-18 (Flash Column, Cat No: CO140080-0, 80 g, 40–60 μm, 60 Å, Agela Technologies) with gradient MeOH/H₂O (20 mL/min) from 10 to 100% (10%, 20%, 30%, 40%, 50%, 60%, 70%, 80%, 90%, 100%) to respectively generate Fr.1–Fr.10. Fr.5 (76 mg) was purified by semi-preparative HPLC to afford **1** (YMC-Pack ODS-A, 3 mL/min, 55% MeCN, t_R=13.3 min, 8.0 mg). Fr.7 (90 mg) was repeatedly purified by semi-preparative HPLC to produce **2** (YMC-Pack ODS-A, 3 mL/min, 55% MeCN, t_R=13.3 min, 8.3 mg) and **3** (YMC-Pack Ph, 3 mL/min, 53% MeCN, t_R=13.9 min, 2.8 mg). Fr.9 (74 mg) was repeatedly purified by semi-preparative HPLC to produce **4** (YMC-Pack ODS-A, 3 mL/min, 94% MeCN, t_R=18.4 min, 12.0 mg). Fr.10 (561 mg) was chromatographed on Sephadex LH-20 (PJLH020, BIOBOMEI) column (size: 3.5×125 cm, CH₂Cl₂-MeOH, v/v, 1:1) to afford eight subfractions Fr.10.1–Fr.10.8. Fr.10.4 (60 mg)

and Fr.10.5 (38 mg) were further purified by semi-preparative HPLC to afford **5** (YMC-Pack ODS-A, 3 mL/min, 94% MeCN, tR=16.6 min, 1.3 mg) and **6** (YMC-Pack ODS-A, 2.5 mL/min, 82% MeOH, tR=9.5 min, 6.7 mg) respectively. Fr.3 (368 mg) was chromatographed on Sephadex LH-20 (PjLH020, BIOBOMEI) column (size: 3.5×125 cm, CH₂Cl₂-MeOH, v/v, 1:1) to afford seven subfractions Fr.3.1–Fr.3.7. Fr.3.2 (40 mg) was further purified by semi-preparative HPLC to afford **7** (YMC-Pack ODS-A, 3 mL/min, 45% MeOH, tR=8.0 min, 2.1 mg).

Monaprenylindole A (**1**): HRESIMS *m/z* 244.1339 [M+H]⁺ (calcd for C₁₅H₁₈NO₂ 244.1332). ¹H NMR (chloroform-*d*, 500 MHz) and ¹³C NMR (chloroform-*d*, 126 MHz), see Fig. S11–S13.

3-Cyanomethyl-6-prenylindole (**2**): red powder, ESIMS *m/z* 225.5 [M+H]⁺, C₁₅H₁₇N₂, ¹H NMR (chloroform-*d*, 500 MHz) and ¹³C NMR (chloroform-*d*, 126 MHz), see Fig. S14–S16.

6-Prenyltryptophol (**3**): red powder, ESIMS *m/z* 230.5 [M+H]⁺, C₁₅H₁₉NO, ¹H NMR (chloroform-*d*, 700 MHz) and ¹³C NMR (chloroform-*d*, 176 MHz), see Fig. S17–S19.

Anthracimycin (**4**): colorless crystal (MeOH-CHCl₂, 1:1), m.p.=151.4~152.9 °C, Flack parameter=-0.07 (11), ESIMS *m/z* 397.7 [M+H]⁺, C₂₅H₃₂O₄, ¹H NMR (chloroform-*d*, 700 MHz) and ¹³C NMR (chloroform-*d*, 176 MHz), see Fig. S20–S22.

2-*Epi*-anthracimycin (**5**): white powder, ESIMS *m/z* 419.7 [M+Na]⁺, C₂₅H₃₂O₄, ¹H NMR (chloroform-*d*, 700 MHz) and ¹³C NMR (chloroform-*d*, 176 MHz), see Fig. S23–S25.

β-Rubromycin (**6**): red powder, ESIMS *m/z* 537.2 [M+H]⁺, C₂₇H₂₀O₁₂, ¹H NMR (chloroform-*d*, 500 MHz) and ¹³C NMR (chloroform-*d*, 126 MHz), see Fig. S26–S28.

4-(Dimethylamino) benzoic acid (**7**): white powder, ESIMS *m/z* 166.2 [M+H]⁺, C₉H₁₁NO₂, ¹H NMR (methanol-*d*₄, 700 MHz) and ¹³C NMR (methanol-*d*₄, 176 MHz), see Fig. S29–S31.

Crystallographic data for the structure of **4** has been deposited in the Cambridge Crystallographic Data Centre (deposition number CCDC2164743).

Antibacterial assays

Initially, antibacterial activities against the bacterial strains (*Bacillus thuringiensis* ATCC 10792, *Staphylococcus aureus* ATCC 29213, *Bacillus subtilis* BS01, *Acinetobacter baumannii* ATCC 19606 and *Escherichia coli* ATCC 25922) were evaluated using the agar well diffusion method [32]. The tested bacterial strains were cultivated in Luria–Bertani (LB) agar plate at 37 °C. Gentamicin sulfate (2 mg/mL) was used as positive control,

methanol as negative control. The eleven EtOAc extracts were dissolved in MeOH at the concentration of 20 mg/mL, the crude extract at concentration of 10 mg/mL, and the ten fractions (Fr.1–Fr.10) at concentration of 4 mg/mL. A 5 μL quantity of tested solution was added in plate agar well of 6 mm diameter punched after LB agar solidification, previously mixed with 100 μL seeded broth cultivated overnight. After 24 h incubation, inhibition zones were measured. Further, the minimum inhibitory concentrations (MICs) were determined using the broth microdilution method [33]. The tested compounds were dissolved in DMSO, and ciprofloxacin hydrochloride was used as positive control, DMSO as negative control. The bacterial suspension's turbidity is adjusted to the McFarland Standard 0.5 approximately equal to 1×10⁸ CFU/mL, and further diluted by a factor of 1:100 by adding 200 μL bacterial suspension to 19.8 mL sterile LB broth in a sterile 50 mL Erlenmeyer flask to prepare a 20 mL inoculum. A 100 μL/well of the diluted inoculum was mixed with 10 μL/well of the tested compound and 90 μL/well of LB broth, resulting in the final desired inoculum of around 5×10⁵ CFU/mL. Each compound was serially diluted in LB broth with a dilution of 1:2 to provide ten different concentrations starting at 32 μg/mL, ending at 0.06 μg/mL. The 96-well microtiter plates were incubated at 37 °C for 16–20 h.

The cytotoxicity assay

Cytotoxicity evaluation of compound **1** against the human tumor cell line HL-60 was determined by CCK-8 assay as described previously [34].

α-Glucosidase inhibition assay

The inhibitory activity of α-glucosidase was measured as previously our paper [34], and the IC₅₀ value was determined using serial twofold dilutions of compounds **1–3** in DMSO to provide five final concentrations starting at 100 μg/mL, yet that of acarbose as positive control starting at 14.3 μg/mL. The assay was performed in triplicate and the IC₅₀ value was calculated by GraphPad Prism 9 software.

Results and discussion

Phylogenetic analysis

The almost complete 16S rRNA gene sequence of strain SCSIO 75703^T was obtained. The 16S rRNA gene sequences similarities of strain SCSIO 75703^T and *S. solaniscabiei* FS70^T, *S. collinus* CGMCC 4.1623^T, *S. violaceochromogenes* CGMCC 4.1753^T and *S. iakyrus* CGMCC 4.1912^T were 98.8%, 98.7%, 98.5% and 98.5%, respectively. Because *S. solaniscabiei* FS70^T is not a valid name, we excluded it from the main analysis. The neighbour-joining phylogenetic tree (Fig. S1) based on

the almost complete 16S rRNA gene sequence showed that strain SCSIO 75703^T was closely related to *S. collinus* CGMCC 4.1623^T. The maximum-likelihood (Fig. S2) and maximum-parsimony algorithms (Fig. S3) also verified this relation. Although these 16S rRNA phylogenetic trees indicate this relationship, the bootstrap value for the branch of strain SCSIO 75703^T is below 70%, suggesting that the relationship shown by the 16S rRNA phylogenetic tree is not stable. The genome phylogenetic tree (Fig. 1) based on 120 single-copy genes showed that

SCSIO 75703^T belongs to the genus *Streptomyces* and showed the closest phylogenetic relationship with *S. flaveolus* JCM 4032^T, *S. ambofaciens* ATCC 23877^T and *S. lienomycini* LMG 20091^T. The values of ANI, AAI and dDDH between the strain SCSIO 75703^T and *S. flaveolus* JCM 4032^T, *S. ambofaciens* ATCC 23877^T and *S. lienomycini* LMG 20091^T were 84.4–85.9%, 81.7–81.8% and 28.7–29.5%, respectively, which are also low obviously the thresholds of Prokaryotes species (Table 1). These data indicated that strain SCSIO 75703^T should represent a novel member of genus *Streptomyces*.

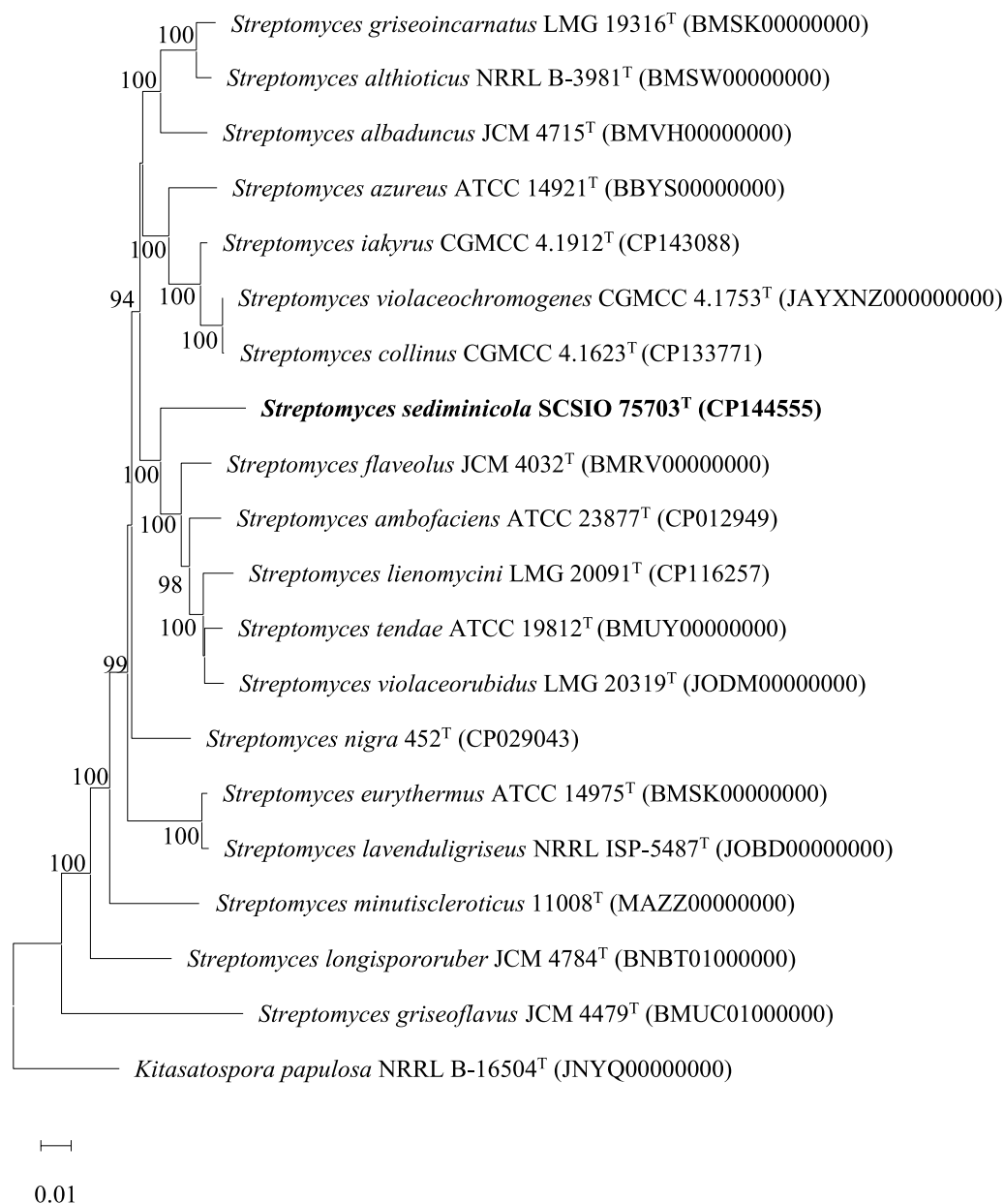


Fig. 1 Phylogenetic analysis based on genome sequences of strains SCSIO 75703^T and its related taxa. *Kitasatospora papulosa* NRRL B-16504^T (JNYQ00000000) was added as an outgroup. Bar, 0.01 substitutions per nucleotide position

Genomic analysis

The genome sizes of SCSIO 75703^T was 6,885,934 bp, with 73.5% DNA G + C content of them (Table S2). A

total of 5,937 genes were predicted from the genome of SCSIO 75703^T, which contained 72 tRNA, 6 5S rRNA, 6 16S rRNA (Similarity, 99.9–100%) and 6 23S rRNA genes (Fig. 2a). The genome completeness of strain SCSIO 75703^T is 99.89% (>95%) with 0.94% contamination (<5%), which was considered as the excellent reference genomes for deeper analyses. Comparative analysis of homologous gene clusters showed that strain 75703^T and its three closely related strains formed 6,515 gene clusters and 3,778 single-copy gene clusters in total (Fig. 2b). The four strains shared 3,885 gene clusters, with the three largest classes associated with hydrolase activity (n=149), molecular function

Table 1 Results of dDDH, ANI, AAI values between strains SCSIO 75703^T and their most closely related species

| Strains | SCSIO 75703 ^T (CP144555) | | |
|--|-------------------------------------|---------|---------|
| | dDDH (%) | ANI (%) | AAI (%) |
| <i>S. flaveolus</i> JCM 4032 ^T (BMRV00000000) | 29.5 | 85.9 | 81.8 |
| <i>S. ambofaciens</i> ATCC 23877 ^T (CP012949) | 28.9 | 85.6 | 81.8 |
| <i>S. lienomycini</i> LMG 20091 ^T (CP116257) | 28.7 | 84.4 | 81.7 |

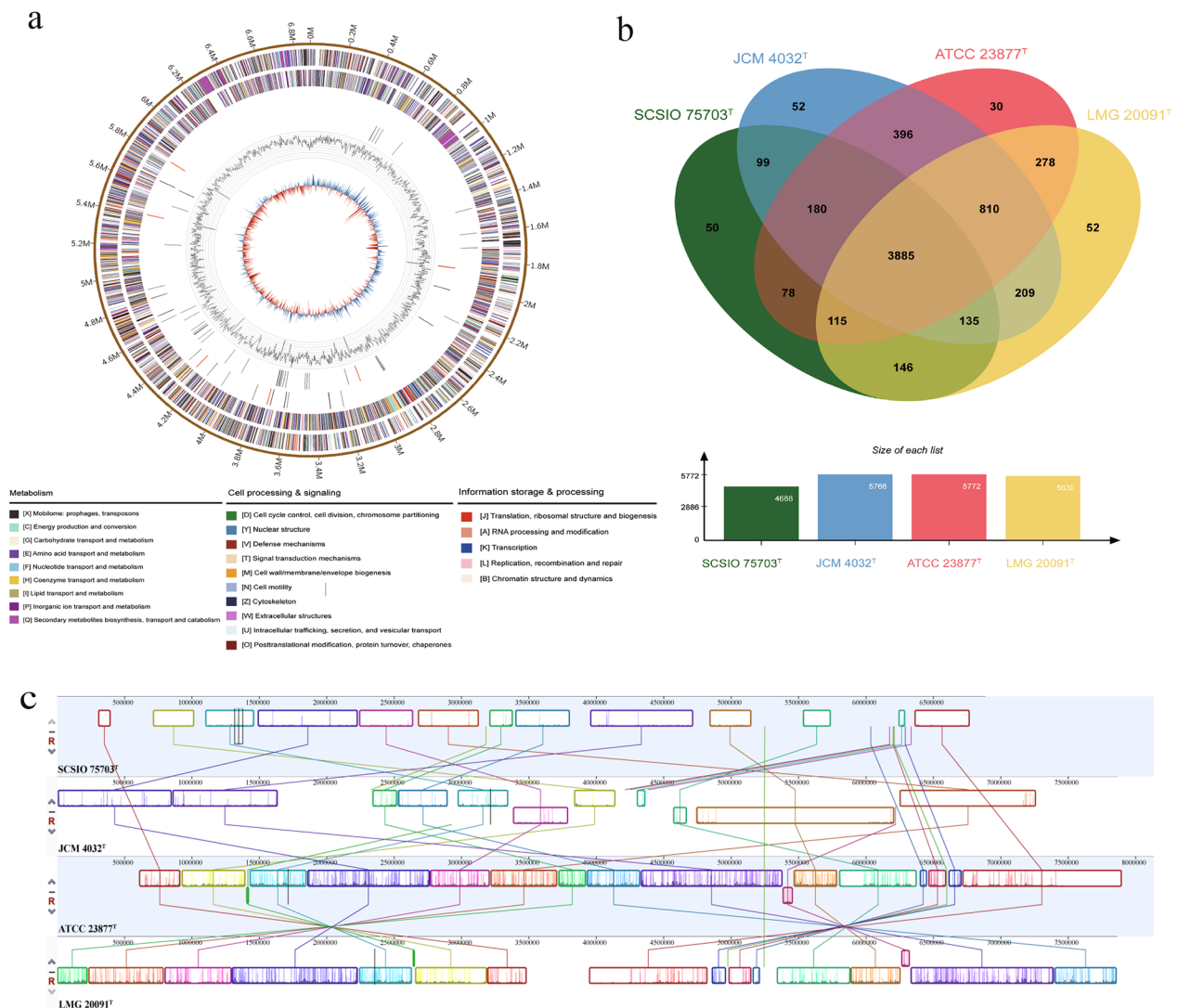


Fig. 2 Comparative genomics analysis. **a** Genome map of strain SCSIO 75703^T. **b** Venn diagram represents the core orthologs and unique genes for strain SCSIO 75703^T and the most closely related strains. **c** Genomic collinearity analysis between strains. Each contiguously colored locally collinear block (LCB) represents a region without rearrangement of the homologous backbone sequence

($n=109$) and oxidoreductase activity ($n=105$). Strain 75703^T shared the most gene clusters ($n=4299$) with *S. flaveolus* JCM 4032^T than with *S. ambofaciens* ATCC 23877^T (4258) and *S. lienomycini* LMG 20091^T (4281). It may be most closely related to *S. flaveolus* JCM 4032^T in physiology. For a more comprehensive genomic comparison, conserved large segment sequence collinear module analysis was performed between the genomes of strain 75703^T and its closely related strains (Fig. 2c). These results showed that the four strains shared many locally collinear blocks, but also showed some large segments of gene rearrangement. These results indicated that although these strains have a very close phylogenetic relationship, there are still significant differences at the genetic level, which is consistent with their being different species.

A total of 25 secondary metabolite biosynthetic gene clusters were predicted, including 13 antibiotic synthesis gene clusters such as streptothritin, collinomycin, anthracomycin, tirandamycin, lomofungin, etc., accounting for 54.2%, indicating that strain SCSIO 75703^T had great potential for synthesis of antibiotics. It also harbours various other secondary metabolite biosynthetic gene clusters, such as terpenes, peptides, polyketides and so on. The secondary metabolite biosynthetic gene clusters of strain SCSIO 75703^T were significantly different from that of its most closely related strains in types and quantity, as shown in Fig. 3 and Table S3.

Phenotypic characteristics

Strain SCSIO 75703^T was Gram-stain-positive and aerobic actinomycetes with spiral spore chains consist of elliptic spores ($0.7\text{--}1.2 \times 0.5\text{--}0.7 \mu\text{m}$) (Fig. S4). Strain SCSIO 75703^T grew well on ISP2, ISP3, ISP4, ISP7, 2216E, NA and TSA medium, but grew weakly on ISP5 and R2A medium (Fig. S5). Growth occurred at 10–37 °C (optimum, 28–35 °C), pH 6.0–10.0 (optimum, pH 7.0–8.0) and 0–10% (w/v) NaCl (optimum, 1.0–3.0%). Cells were catalase positive and oxidase negative. Strain SCSIO 75703^T was positive for hydrolysis of Tween 80, gelatin and starch, but negative for hydrolysis of Tweens 20, 40, 60, cellulose, coagulation and peptonization of milk. Differences between strain SCSIO 75703^T and the closely related reference strains include variations in optimum temperature, pH, NaCl range, the ability to hydrolysis of Tweens, utilization of carbohydrates and enzymatic activities, etc. (Table S4).

Chemotaxonomic characterization

The major cellular fatty acids (>10%) of strain SCSIO 75703^T were identified as iso- $C_{16:0}$, iso- $C_{15:0}$ and anteiso- $C_{15:0}$. The predominant fatty acid was iso- $C_{16:0}$, which was consistent with the reference strains shown in Table S5. The predominant menaquinones of strain SCSIO 75703^T were MK-10(H_{10}) (74.7%) and MK-10(H_8) (25.3%). *LL*-2,6-Diaminopimelic acid was identified as the cell-wall diamino acid. The whole-cell sugars included galactose, glucose and ribose. The polar lipids comprised

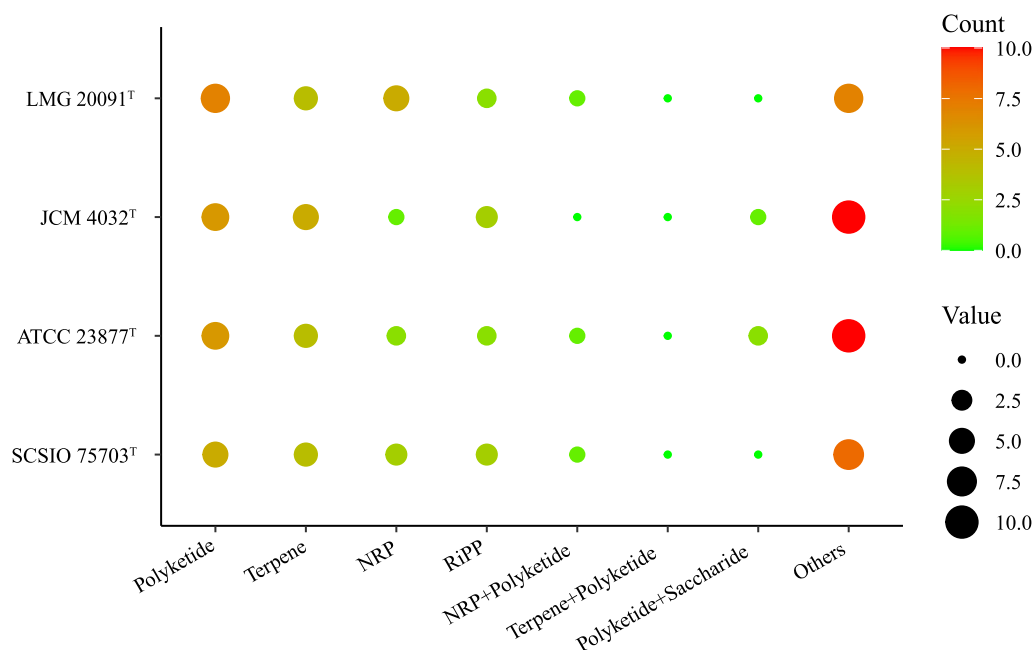


Fig. 3 Biosynthetic gene cluster types of strain SCSIO 75703^T and most closely related strains. The values of the size of each circle represent the number of different types of secondary metabolite biosynthetic gene clusters

diphosphatidylglycerol (DPG), phosphatidylethanolamine (PE), phosphatidylmethylethanolamine (PME), one unidentified amino phospholipid (APL), three unidentified phospholipids (PL) and one unidentified lipid (L) (Fig. S6).

Antibacterial activity-oriented separation

To fully uncover the secondary metabolites and biological activities of strain SCSIO 75703^T, small amounts of fermentation were performed on eleven different media (Table S1) based on OSMAC strategy. The similar profiles appeared in HPLC–UV analytic chromatogram (Fig. S7) were further observed in the eleven EtOAc extracts. All of eleven extracts displayed obvious antibacterial activities against *B. thuringiensis* ATCC 10792, *S. aureus* ATCC 29213 and *B. subtilis* BS01, but not against *E. coli* ATCC 25922 using the agar well diffusion method at the concentration of 20 mg/mL (Table 2).

The MC3 medium was selected for large-scale fermentation due to the more abundant metabolic profiles observed in the HPLC–UV analytic chromatogram (Fig. S7–S8). A total of 30 L broth was fermented in the shaking flask, and the EtOAc extract was obtained from the fermentation liquor. The antibacterial assay was carried out for ten fractions Fr.1–Fr.10 isolated from the crude extract, and the result was listed in Table 3. The result showed that the first six fractions (Fr.1–Fr.6) did not display antibacterial effect, but the next four fractions (Fr.7–Fr.10) exhibited obvious inhibitory activity against the above four bacteria with inhibition zones of 0.8~1.5 cm at lower concentration of 4 mg/mL. The same metabolic

Table 2 Antibacterial activities of eleven extracts

| Sample | <i>B. thuringiensis</i> ATCC 10792 | <i>S. aureus</i> ATCC 29213 | <i>B. subtilis</i> BS01 | <i>E. coli</i> ATCC 25922 |
|-------------------------|---------------------------------------|--------------------------------|-------------------------|------------------------------|
| 2216E | +++ | +++ | ++ | - |
| MC3 | +++ | ++++ | + | - |
| MRA | ++ | +++ | ++ | - |
| MA | ++ | +++ | ++ | - |
| M2216E | ++ | +++ | ++ | - |
| MISP2 | ++ | +++ | ++ | - |
| MM18 | ++ | +++ | + | - |
| AM3 | ++ | +++ | ++ | - |
| MJNP1A | ++ | ++ | ++ | - |
| MK | ++ | +++ | + | - |
| MISP4 | ++ | ++ | ++ | - |
| Gentamicin ^a | ++ | +++ | ++++ | - |

^a Gentamicin is used as positive control at the concentration of 2 mg/mL (5 μ L), and methanol is used as negative control

+, ++, +++ and ++++ represent zone of inhibition of 6–10 mm, 11–15 mm, 16–20 mm and 21–25 mm, respectively; and the well diameter with 6 mm

Table 3 Antibacterial activities of different fractions

| Sample | <i>B. thuringiensis</i> ATCC 10792 | <i>S. aureus</i> ATCC 29213 | <i>B. subtilis</i> BS01 |
|--------------------------------|---------------------------------------|--------------------------------|-------------------------|
| The crude extract ^a | ++ | ++ | ++ |
| Fr.1–Fr.6 | - | - | - |
| Fr.7 | + | + | + |
| Fr.8 | + | - | ++ |
| Fr.9 | + | + | ++ |
| Fr.10 | ++ | ++ | ++ |
| Gentamicin ^a | ++ | +++ | ++++ |

^a The crude extract at 10 mg/mL (5 μ L)

^b Gentamicin at the concentration of 2 mg/mL (5 μ L). Fr.1–Fr.10 at 4 mg/mL (5 μ L)

- represents no inhibitory activity

+, ++, +++ and ++++ represent zone of inhibition of 6–10 mm, 11–15 mm, 16–20 mm and 21–25 mm, respectively; and the well diameter with 6 mm

profiles were observed in HPLC chromatogram at 19.7 min for Fr.7–Fr.10 and 36 min for Fr.9 and Fr.10 (Fig. S9), which were further identified as β -rubromycin (6) and anthracimycin (4) respectively. In agreement with the above result, both of the two monomeric compounds exhibited potent inhibitory effect against Gram-positive bacteria in accordance with that previous reported.

Structural elucidation

The isolated compounds (Fig. 4) were elucidated by comparison of their spectra data with those described in the literatures. Compounds 1–3 were identified as monaprenylindole A (1) [35], 3-cyanomethyl-6-prenylindole (2) [36] and 6-prenyltryptophol (3) [36]. Compounds 4 and 5 were respectively assigned as anthracimycin (4) [37] and 2-*epi*-anthracimycin (5) [38], in which compound 4 was confirmed for the first time through single-crystal X-ray diffraction analysis using Cu K α radiation (Fig. S10). Other compounds were identified as β -rubromycin (6) [39] and 4-(dimethylamino)benzoic acid (7) [40] by comparison of their spectra data with those described in the literatures.

These compounds were corresponding to the three secondary metabolite biosynthetic gene clusters (BGCs) of indole (gene cluster 24, for compounds 1–3), TransAT-PKS (gene cluster 21, for compounds 4 and 5), and a T2PKS (gene cluster 16, for compound 6) [41], and compound 7 might belong to other secondary metabolite BGCs with unknown functions. Although both gene clusters 13 and 16 belong to the T2PKS, genomic analysis results show that gene cluster 16 shares 96% similarity with the secondary metabolite BGC of collinomycin (synonyms: α -Rubromycin), whereas gene cluster 13 only has 24%. Therefore, we inferred that gene cluster 16 might be responsible for the biosynthesis of compound

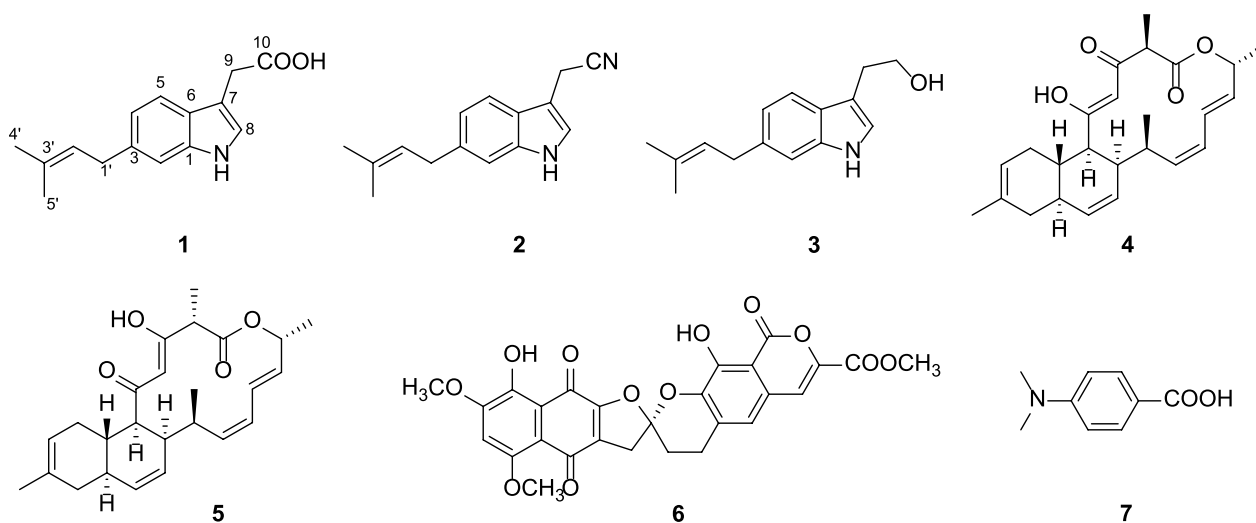


Fig. 4 Structures of compounds 1–7 isolated from strain SCSIO 75703^T

6. Chemical structures and corresponding secondary metabolite BGCs were shown in Fig. 5. Specific secondary metabolite BGCs of strain SCSIO 75703^T were shown in the Table S3. Detailed HPLC analysis revealed the presentation of some unseparated UV-profiles at 0~15 min and 25~35 min (Fig. S8), together with other 22 unexplained BGCs, suggesting that further investigation of this strain is warranted.

Biological activities

The antibacterial assay of compounds 4–6 was assessed using the broth microdilution method [33] against a panel of pathogenic bacteria consisting of five Gram-positive bacteria (*B. subtilis* BS01, *S. aureus* ATCC 29213, *B. thuringiensis* ATCC 10792, *Exiguobacterium profundum* DH012, *Enterococcus faecalis* ATCC 29212) and two Gram-negative bacteria (*A. baumannii* ATCC 19606, *Vibrio alginolyticus* XSBZ14). Notably, compounds 4–6, especially 4 and 6 displayed strong antibacterial activities against five Gram-positive

bacteria with minimum inhibitory concentrations (MICs) of ≤ 16 $\mu\text{g}/\text{mL}$, which was consistent with the result of bioassay-guided fractionation (Table 4). Additionally, anthracimycin (4) and β -rubromycin (6) exhibited a better antibacterial effect against four Gram-positive bacteria (*S. aureus* ATCC 29213, *B. thuringiensis* ATCC 10792, *Eb. Profundum* DH012 and *Ec. faecalis* ATCC 29212) than ciprofloxacin, and that of β -rubromycin (6) was equal to ciprofloxacin against *B. subtilis* BS01. Meanwhile, compared to anthracimycin (4), 2-*epi*-anthracimycin (5) displayed much weaker antibacterial activity against five Gram-positive bacteria, suggesting that anthracimycin was still more potent antibiotics among its analogues. However, the three compounds were inactive against two Gram-negative bacteria with MIC values of > 32 $\mu\text{g}/\text{mL}$.

Meanwhile, compound 1 was tested for cytotoxicity against HL-60 human tumor cell line by WST-8 reagent, resulting in no obvious inhibitory activity at concentration of 100 μM . In addition, all compounds were

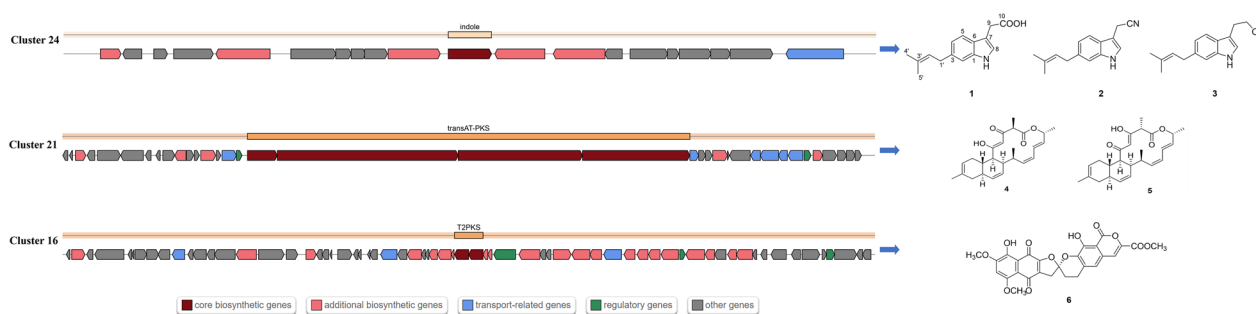


Fig. 5 Chemical structures and corresponding biosynthetic gene clusters in strain SCSIO 75703^T

Table 4 The antibacterial activities of compounds 4–6

| | MICs ($\mu\text{g/mL}$) | Anthracimycin (4) | 2- <i>epi</i> -anthracimycin (5) | β -rubromycin (6) |
|------------------------------------|---------------------------|-------------------|----------------------------------|-------------------------|
| Bacteria | | | | |
| <i>B. subtilis</i> BS01 | 2 | 4 | 1 | 1 |
| <i>S. aureus</i> ATCC 29213 | 0.125 | 8 | 0.125 | 0.5 |
| <i>B. thuringiensis</i> ATCC 10792 | 0.125 | 8 | 0.125 | 1 |
| <i>Eb. Profundum</i> DH012 | 0.125 | 4 | 0.5 | 1 |
| <i>Ec. faecalis</i> ATCC 29212 | 0.25 | 16 | 0.5 | 1 |
| <i>A. baumannii</i> ATCC 19606 | > 32 | > 32 | > 32 | 1 |
| <i>V. alginolyticus</i> XSBZ14 | > 32 | > 32 | > 32 | 1 |

^a Ciprofloxacin is used as positive control

Table 5 Inhibitory activity of the compounds 1–3 and acarbose against α -glucosidase (n=3)

| Compounds | IC ₅₀ ($\mu\text{g/mL}$) ^a |
|-----------------------|--|
| 1 | 83.27 |
| 2 | 86.21 |
| 3 | 45.4% inhibition at 100 $\mu\text{g/mL}$ |
| Acarbose ^b | 2.32 |

^a IC₅₀ is the concentration producing 50% inhibition of the enzyme activity

^b Acarbose is used as a positive control

measured for α -glucosidase inhibitory activity in vitro. We also discovered that compounds 1–3 were able to inhibit to a certain extent α -glucosidase in a concentration-dependent way. Furtherly, compounds 1 and 2 exhibited moderate inhibitory effect with the IC₅₀ values of 83.27 and 86.21 $\mu\text{g/mL}$, respectively (Table 5).

Conclusion

These results from the 16S rRNA gene similarity, ANI, AAI, dDDH values, phylogenetic, phenotypic and chemotaxonomic analyses indicate that strain SCSIO 75703^T represents a novel species within the genus *Streptomyces*, for which the name *Streptomyces sediminicola* sp. nov. is proposed. The OSMAC strategy proved to be a simple yet efficient method for primarily exploring the metabolic profiles in association with HPLC chromatography. In combination with bioassay-guided fractionation, seven compounds (1–7) were isolated and identified from strain SCSIO 75703^T using extensive spectroscopic analyses based on the above strategy in the present paper. Besides, bioactive assay demonstrated that compounds 4–6, especially anthracimycin (4) and β -rubromycin (6) possessed potent antibacterial activities against five Gram-positive bacteria with the MIC values of 0.125–16 $\mu\text{g/mL}$, and compounds 1 and 2 exhibited α -glucosidase inhibition

activities with the IC₅₀ values of 83.27 and 86.21 $\mu\text{g/mL}$ respectively. Anthracimycin as a promising drug lead has received great attention due to its outstanding antimicrobial activity, inducing the increasing interest to discover the high-producer of anthracimycin and more bioactive analogues [42]. Moreover, prenylated indole alkaloids presented different biological activity in various side chain of indole according to the reported reference [36]. Meanwhile, the detective HPLC–UV profiles revealed that the strain predominantly synthesized anthracimycin, β -rubromycin, prenylated indole alkaloids and a small amount of 2-*epi*-anthracimycin in multiple media. suggesting that the strain has the potential to become a new natural producer of anthracimycin, but it remains to be studied in future.

Description of *Streptomyces sediminicola* sp. nov.

Streptomyces sediminicola (se.di.mi.ni'co.la. L. neut. n. *sedimen -inis*, sediment; L. masc./fem. n. suff. *-cola*, inhabitant, dweller; N.L. masc./fem. n. *sediminicola*, sediment-dweller, pertaining to the sea sediment from which the type strain was isolated).

Cells are Gram-stain-positive and aerobic actinomycetes with spiral spore chains consist of elliptic spores. Growth occurs well on ISP2, ISP3, ISP4, ISP7, 2216E, NA and TSA medium, but weakly on ISP5 and R2A medium. Growth occurs at 10–37 °C (optimum, 28–35 °C), pH 6.0–10.0 (optimum, pH 7.0–8.0) and 0–10% (w/v) NaCl (optimum, 1.0–3.0%). Cells are catalase positive and oxidase negative. Cells are positive for hydrolysis of Tweens 80, gelatin and starch, but negative for hydrolysis of Tween 20, 40, 60, cellulose, coagulation and peptonization of milk. The major cellular fatty acids (> 10%) are iso-C_{15:0}, iso-C_{16:0} and anteiso-C_{15:0}. The cell-wall diamino acid was LL-2,6-Diaminopimelic acid. The whole-cell sugars are galactose, glucose and ribose. The polar lipids are diphosphatidylglycerol, phosphatidylethanolamine, phosphatidylmethylethanolamine, one unidentified amino phospholipid,

three unidentified phospholipids and one unidentified lipid. The predominant menaquinones are MK-10(H₈) and MK-10(H₁₀). The type strain is SCSIO 75703^T (=MCCC 1.17019^T = AKM 43091^T).

Supplementary Information

The online version contains supplementary material available at <https://doi.org/10.1186/s12934-024-02558-z>.

Additional file 1.

Acknowledgements

The authors also appreciate the analytical facility center (Zhihui Xiao, Xiaohong Zheng, Aijun Sun, Xuan Ma and Yun Zhang) in the analytical facilities of the South China Sea Institute of Oceanology, Chinese Academy of Sciences.

Author contributions

K. Z. and WP. D. performed the experiments and wrote the manuscript; Sb. S. helped with formal analysis; L.J. L. offer resources. H. Y. helped with supervision; writing—review and editing; XP. T. helped with conceptualization; supervision; writing—review and editing. All authors have read and agreed to the published version of the manuscript.

Funding

The authors are grateful for the financial support provided by the National Key Research and Development Program of China (2022YFC3103601), the Science and Technology Planning Project of Guangdong Province of China (2021B1212050023) and Key-Area Research and Development Program of Guangdong Province (2020B1111030004).

Data availability

No datasets were generated or analysed during the current study.

Declarations

Ethics approval and consent to participate

Not applicable.

Consent for publication

All authors agreed to publish this article.

Competing interests

The authors declare no competing interests.

Author details

¹CAS Key Laboratory of Tropical Marine Bio-Resources and Ecology, South China Sea Institute of Oceanology, Chinese Academy of Sciences, Guangzhou 510301, China. ²CAS Key Laboratory of Quantitative Engineering Biology, Shenzhen Institute of Synthetic Biology, Shenzhen Institutes of Advanced Technology, Chinese Academy of Sciences, Shenzhen 518055, China. ³Guangdong Provincial Observation and Research Station for Coastal Upwelling Ecosystem, South China Sea Institute of Oceanology, Chinese Academy of Sciences, Shantou 515041, China.

Received: 8 May 2024 Accepted: 6 October 2024

Published online: 19 October 2024

References

- Fenical W, Jensen PR. Developing a new resource for drug discovery: marine actinomycete bacteria. *Nat Chem Biol*. 2006;2:666–73.
- Shen B. A new golden age of natural products drug discovery. *Cell*. 2015;163:1297–300.
- Islam MM, Tan Y, Hameed HMA, Chhotaray C, Liu Z, Liu Y, Lu Z, Wang S, Cai X, Gao Y, et al. Phenotypic and genotypic characterization of streptomycin-resistant multidrug-resistant *Mycobacterium tuberculosis* clinical isolates in Southern China. *Microb Drug Resist*. 2020;26:766–75.
- Subramani R, Sipkema D. Marine rare actinomycetes: a promising source of structurally diverse and unique novel natural products. *Mar Drugs*. 2019;17(15):249.
- Donald L, Pipite A, Subramani R, Owen J, Keyzers RA, Taufat T. *Streptomyces*: still the biggest producer of new natural secondary metabolites, a current perspective. *Microbiol Res*. 2022;13:418–65.
- Lacey HJ, Rutledge PJ. Recently discovered secondary metabolites from *Streptomyces* species. *Molecules*. 2022;27:887.
- Yang Z, He J, Wei X, Ju J, Ma J. Exploration and genome mining of natural products from marine *Streptomyces*. *Appl Microbiol Biotechnol*. 2020;104:67–76.
- Dharmaraj S. Marine *Streptomyces* as a novel source of bioactive substances. *World J Microbiol Biotechnol*. 2010;26:2123–39.
- Barka EA, Vatsa P, Sanchez L, Gaveau-Vaillant N, Jacquard C, Meier-Kolthoff JP, Klenk HP, Clément C, Ouhdouch Y, van Wezel GP. Taxonomy, physiology, and natural products of actinobacteria. *Microbiol Mol Biol Rev*. 2016;80:1–43.
- Li WJ, Xu P, Schumann P, Zhang YQ, Pukall R, Xu LH, Stackebrandt E, Jiang CL. *Georgenia ruanii* sp. nov., a novel actinobacterium isolated from forest soil in Yunnan (China), and emended description of the genus *Georgenia*. *Int J Syst Evol Microbiol*. 2007;57:1424–8.
- Yoon SH, Ha SM, Kwon S, Lim J, Kim Y, Seo H, Chun J. Introducing EzBioCloud: a taxonomically united database of 16S rRNA gene sequences and whole-genome assemblies. *Int J Syst Evol Microbiol*. 2017;67:1613–7.
- Saitou N, Nei M. The neighbor-joining method: a new method for reconstructing phylogenetic trees. *Mol Biol Evol*. 1987;4:406–25.
- Felsenstein J. Evolutionary trees from DNA sequences: a maximum likelihood approach. *J Mol Evol*. 1981;17:368–76.
- Fitch WM. Toward defining the course of evolution: minimum change for a specific tree topology. *Syst Biol*. 1971;20:406–16.
- Tamura K, Stecher G, Kumar S. MEGA11: molecular evolutionary genetics analysis version 11. *Mol Biol Evol*. 2021;38:3022–7.
- Wick RR, Judd LM, Gorrie CL, Holt KE. Unicycler: Resolving bacterial genome assemblies from short and long sequencing reads. *PLoS Comput Biol*. 2017;13: e1005595.
- Parks DH, Imelfort M, Skennerton CT, Hugenholtz P, Tyson GW. CheckM: assessing the quality of microbial genomes recovered from isolates, single cells, and metagenomes. *Genome Res*. 2015;25:1043–55.
- Yoon SH, Ha SM, Lim J, Kwon S, Chun J. A large-scale evaluation of algorithms to calculate average nucleotide identity. *Antonie Van Leeuwenhoek*. 2017;110:1281–6.
- Meier-Kolthoff JP, Carbasse JS, Peinado-Olarte RL, Göker M. TYGS and LPSN: a database tandem for fast and reliable genome-based classification and nomenclature of prokaryotes. *Nucleic Acids Res*. 2021;50:D801–7.
- Rodriguez LM, Konstantinidis KT. The enveomics collection: a toolbox for specialized analyses of microbial genomes and metagenomes. 2016.
- Chaumeil PA, Mussig AJ, Hugenholtz P, Parks DH. GTDB-Tk: a toolkit to classify genomes with the genome taxonomy database. *Bioinformatics*. 2019;36:1925–7.
- Sun J, Lu F, Luo Y, Bie L, Xu L, Wang Y. OrthoVenn3: an integrated platform for exploring and visualizing orthologous data across genomes. *Nucleic Acids Res*. 2023;51:W397–403.
- Darling AE, Mau B, Perna NT. progressiveMauve: multiple genome alignment with gene gain, loss and rearrangement. *PLoS ONE*. 2010;5: e11147.
- Blin K, Shaw S, Augustijn HE, Reitz ZL, Biermann F, Alanjary M, Fetter A, Terlouw BR, Metcalf WW, Helfrich EJM, et al. antiSMASH 7.0: new and improved predictions for detection, regulation, chemical structures and visualisation. *Nucleic Acids Res*. 2023; 51:46–50.
- Leifson E. *Atlas of bacterial flagellation*. New York: Academic Press; 1960.
- Gonzalez C, Gutierrez C, Ramirez C. *Halobacterium vallismortis* sp. nov. An amyolytic and carbohydrate-metabolizing, extremely halophilic bacterium. *Can J Microbiol*. 1978;24:710–5.
- Collins MD, Pirouz T, Goodfellow M, Minnikin DE. Distribution of Menaquinones in *Actinomycetes* and *Corynebacteria*. *Microbiology*. 1977;100:221–30.
- Tamaoka J, Katayama-Fujimura Y, Kuraishi H. Analysis of bacterial menaquinone mixtures by high performance liquid chromatography. *J Appl Bacteriol*. 1983;54:31–6.

29. Lechevalier HA, Lechevalier MP, Gerber NN. Chemical Composition as a Criterion in the Classification of Actinomycetes. *Adv Appl Microbiol.* 1971;14:47–72.
30. Stanek JL, Roberts GD. Simplified Approach to Identification of Aerobic Actinomycetes by Thin-Layer Chromatography. *Appl Microbiol.* 1974;28:226–31.
31. Minnikin DE, O'Donnell AG, Goodfellow M, Alderson G, Athalye M, Schaal A, Parlett JH. An integrated procedure for the extraction of bacterial isoprenoid quinones and polar lipids. *J Microbiol Methods.* 1984;2:233–41.
32. Yin S, Liu Z, Shen J, Xia Y, Wang W, Gui P, Jia Q, Kachanuban K, Zhu W, Fu P. Chimeric natural products derived from medermycin and the nature-inspired construction of their polycyclic skeletons. *Nat Comm.* 2022;13:5169.
33. Wiegand I, Hilpert K, Hancock REW. Agar and broth dilution methods to determine the minimal inhibitory concentration (MIC) of antimicrobial substances. *Nature Protocols.* 2008;3:163–75.
34. Ding W, Li Y, Chen M, Chen R, Tian X, Yin H, Zhang S. Structures and antitumor activities of ten new and twenty known surfactins from the deep-sea bacterium *Limimarincola* sp. SCSIO 53532. *Bioorg Chem.* 2022;120:105589.
35. Yi W, Ge Z-W, Wu B, Zhang Z. New metabolites from the marine-derived bacterium *Pseudomonas* sp. ZZ820R. *Fitoterapia.* 2020;143:104555.
36. Sánchez López JM, Martínez Insua M, Pérez Baz J, Fernández Puentes JL, Cañedo Hernández LM. New Cytotoxic Indolic Metabolites from a Marine *Streptomyces*. *J Nat Prod.* 2003;66:863–4.
37. Jang KH, Nam SJ, Locke JB, Kauffman CA, Beatty DS, Paul LA, Fenical W. Anthracimycin, a Potent Anthrax Antibiotic from a Marine-Derived Actinomycete. *Angew Chem Int Ed.* 2013;52:7822–4.
38. Fukuda T, Nagai K, Kanamoto A, Tomoda H. 2-*Epi*-anthracimycin, a new cytotoxic agent from the marine-derived actinomycete *Streptomyces* sp. OPMA00631. *J Antibiot.* 2020;73:548–53.
39. Puder C, Loya S, Hizi A, Zeeck A. Structural and Biosynthetic Investigations of the Rubromycins. *Eur J Org Chem.* 2000;2000:729–735.
40. Catbagan C. New sirtuin inhibitors from marine-derived actinomycetes. Masters Thesis. San Francisco State University. Chemistry. 2016.
41. Atkinson DJ, Brimble MA. Isolation, biological activity, biosynthesis and synthetic studies towards the rubromycin family of natural products. *Nat Prod Rep.* 2015;32:811–840.
42. Sirota FL, Goh F, Low K-N, Yang L-K, Crasta SC, Eisenhaber B, Eisenhaber F, Kanagasundaram Y, Ng SB. Isolation and identification of an anthracimycin analogue from *Nocardiopsis kunsanensis*, a halophile from a saltern, by genomic mining strategy. *J Genom.* 2018;6:63–73.

Publisher's Note

Springer Nature remains neutral with regard to jurisdictional claims in published maps and institutional affiliations.